JOURNAL OF MATERIALS SCIENCE **39** (2004) 1061 – 1063

Influence of a finite notch root radius on the measured R-curves

T. FETT
Forschungszentrum Karlsruhe, Institut für Materialforschung II, Postfach 3640, D-76021 Karlsruhe, Germany
E-mail: theo.fett@imf.fzk.de

Most R-curve investigations on ceramics deal with cracks starting from narrow notches. These are introduced in test specimens by thin saw cuts or produced with the razor blade procedure as proposed by Nishida *et al.* [1] and successfully applied by Kübler [2]. If a_0 is the depth of the notch and ℓ the length of an edge crack propagating from the notch root (for the geometric data see Fig. 1a), the stress intensity factor commonly is formally computed as the stress intensity factor for a crack of total length $a_0 + \ell$, i.e.,

$$K^* = \sigma_{\mathrm{bend}}\sqrt{\pi(a_0+\ell)}\,F_{\mathrm{bend}}(a/W) \tag{1}$$

where F_{bend} is the geometric function for an edge crack of length $a = a_0 + \ell$ in a specimen of width W under the applied load, here, for instance, under bending load. The geometric function is available from fracture mechanics handbooks.

The stress intensity factor K^* given by Equation 1, of course, is the correct value in cases of the crack length ℓ being clearly larger than the radius of the notch. In the first crack extension phase, where the crack length ℓ is comparable to R, the quantity K^* deviates strongly from the correct stress intensity factor K. In this case, the fracture mechanics problem of a small crack in front of a finite notch has to be considered. In the special case of an edge crack ahead of a slender notch with R being small compared to the notch depth a_0 and the other specimen dimensions, the true stress intensity factor K is given by [3]

$$K/K^* \cong \tanh[2.243\sqrt{\ell/R}] \tag{2}$$

This relation, successfully applied for fracture toughness evaluation [2, 4–6], is shown in Fig. 1b. From this plot, it is clearly visible that the true stress intensity factor is significantly lower than the formally computed values K^*. On the other hand, it can be concluded from Fig. 1b that notch effects are of importance for $\ell < 1.5R$ only.

In a material with an R-curve effect, the externally applied stress intensity factor K_{appl} and the intrinsic shielding stress intensity factor K_{sh} have to be superimposed in order to obtain the total stress intensity factor K_{total}

$$K_{\mathrm{total}} = K_{\mathrm{appl}} + K_{\mathrm{sh}} \tag{3}$$

which governs the crack tip stress field and is responsible for crack growth. Fig. 2a represents these stress intensity factor contributions as functions of crack extension $\Delta a = \Delta\ell$. Stable crack propagation occurs under the condition of the total stress intensity factor equalling the so-called crack tip toughness K_{I0}

$$K_{\mathrm{total}} = K_{\mathrm{I0}} \tag{4}$$

The influence of the notch effect on the R-curve in terms of $K^*_{\mathrm{appl}} = f(\Delta a)$ or $K^*_{\mathrm{appl}} = f(\Delta\ell)$, here denoted as the "apparent R-curve," will be outlined in the following considerations.

In order to study the influence of a notch on the "apparent R-curve", two different types of shielding stress intensity factors are chosen. A "steep" R-curve may be modelled by the shielding term

$$K_{\mathrm{sh}} = K_{\mathrm{sh,max}}[1 - \exp(-\lambda\sqrt{\Delta a})] \tag{5}$$

which depends on the crack increment Δa. This relation, denoted in the following considerations as "R-curve I", interpolates the square-root-shaped limit case for small crack extensions

$$K_{\mathrm{sh}} \propto \sqrt{\Delta a} \quad \text{for } \Delta a \to 0 \tag{6}$$

and the saturation behavior

$$K_{\mathrm{sh}} \to K_{\mathrm{sh,max}} \quad \text{for } \Delta a \to \infty \tag{7}$$

As a second possibility, an initially linear R-curve may be chosen as

$$K_{\mathrm{sh}} = K_{\mathrm{sh,max}}[1 - \exp(-\beta\Delta a)] \tag{8}$$

denoted as "R-curve II", which interpolates the limit case for small crack extensions

$$K_{\mathrm{sh}} \propto \Delta a \quad \text{for } \Delta a \to 0 \tag{9}$$

and again $K_{\mathrm{sh}} = K_{\mathrm{sh,max}}$ for large crack extension.

The curves related to the chosen parameters of $\lambda = 40/\sqrt{\mathrm{m}}$, $\beta = 1500/\mathrm{m}$, and $K_{\mathrm{sh,max}} = -5\ \mathrm{MPa}\sqrt{\mathrm{m}}$ are given in Fig. 2b. As realistic notch/specimen dimensions $W = 4$ mm and $a_0 = 2$ mm are used for the numerical computations. For the crack tip toughness, let us use $K_{\mathrm{I0}} = 2.4\ \mathrm{MPa}\sqrt{\mathrm{m}}$ as found in [7] for alumina.

The initial crack size ℓ_0 can be estimated by comparing the crack tip toughness K_{I0} obtained from the near-tip crack opening displacement field of a grown crack with the result of strain gauge-equipped notched

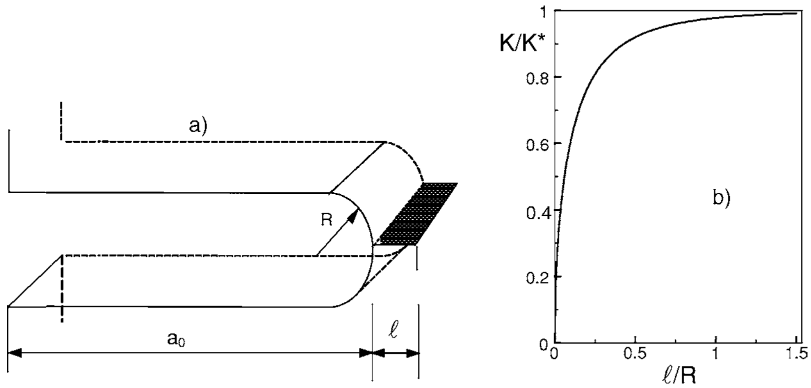

Figure 1 Crack ahead of a slender notch: (a) geometric data and (b) true stress intensity factor.

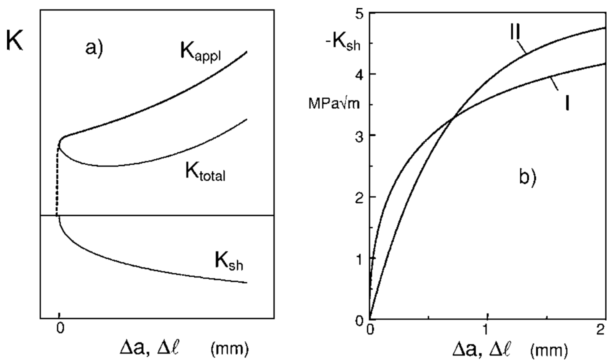

Figure 2 (a) Total stress intensity factor obtained by superposition of the applied and the shielding stress intensity factors according to Equation 3 and (b) shielding stress intensity factors according to Equation 5, "R-curve I" and Equation 8, "R-curve II".

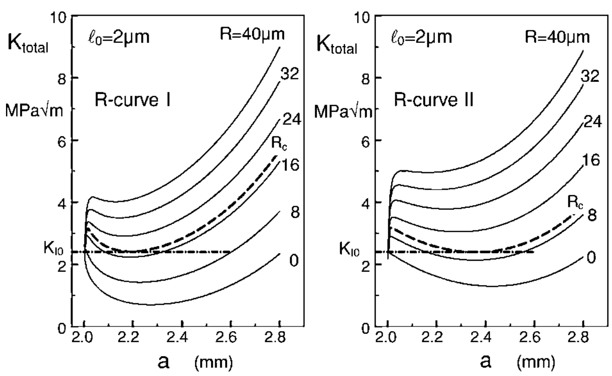

Figure 3 Influence of the notch radius on the total stress intensity factor.

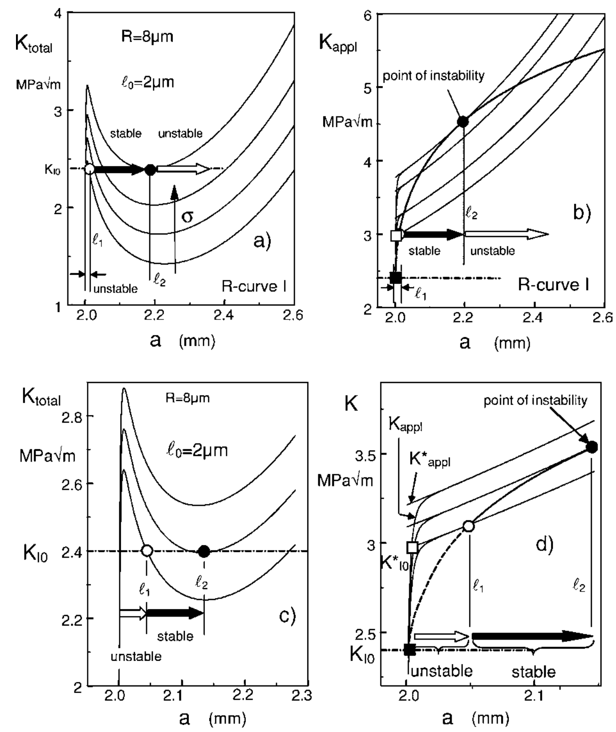

Figure 4 Crack development for an intermediate notch radius of $R = 8$ μm.

bending bars [7]. Depending on the specially assumed crack type, values in the order of $\ell_0 = 2$–5 μm were found for alumina.

The influence of the notch root radius on the total stress intensity factor is illustrated in Fig. 3 for an initial crack size of $\ell_0 = 2$ μm and the two types of R-curve. Since for "R-curve I" an intersection between K_{total} and K_{I0} is obtained for $R < 18$ μm only, this radius denoted as R_c is a limit for reaching stable crack extension. If $R > R_c$, *unstable* crack extension must occur when $K_{\text{total}} = K_{I0}$ is reached for the first time. In the case of R-curve II, the limit radius is about $R_c = 10$ μm.

The different crack extension phases are illustrated in Fig. 4 for a notch radius of $R = 8$ μm $< R_c$ and an initial crack size of $\ell_0 = 2$ μm. Fig. 4a and c show the total stress intensity factors during crack extension, Fig. 4b and d the related R-curves.

A crack of length ℓ_0 starts to propagate, if the condition $K_{\text{total}} = K_{I0}$ is fulfilled for the first time (Fig. 4a and c). The starting point of the "apparent R-curve", the "apparent crack tip toughness" K^*_{I0}, is given as

$$K^*_{I0} = \frac{K_{I0}}{\tanh(2.24\sqrt{\ell_0/R})} \tag{10}$$

resulting in $K^*_{I0} \cong 3$ MPa$\sqrt{\text{m}}$ (open squares in Fig. 4b and d) which is clearly larger than the true crack tip toughness $K_{I0} = 2.4$ MPa$\sqrt{\text{m}}$ (solid squares).

At a second crack length ℓ_1, the condition $K_{\text{total}} = K_{I0}$ is fulfilled again. Between the two crack lengths ℓ_0 and ℓ_1, spontaneous crack extension occurs, followed by stable crack extension from ℓ_1 to ℓ_2 under increased load. At crack length ℓ_2, the curves $K_{I0} =$ constant and $K_{\text{total}}(a)$ have the same horizontal tangent. For $\ell > \ell_2$ the specimen fails by spontaneous crack growth.

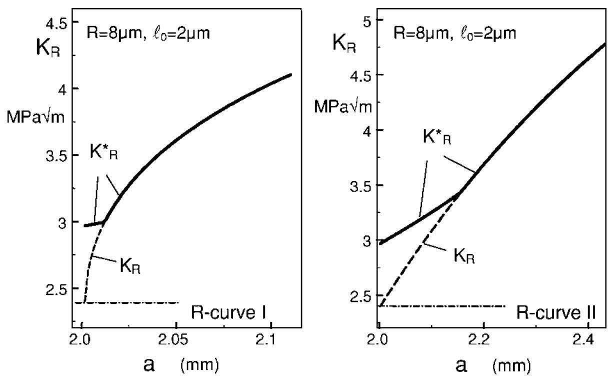

Figure 5 Comparison of the apparent R-curves $K^*(\Delta a)$ for an intermediate notch root radius (solid curve) with the true R-curve (dashed curve).

The initial dashed parts of the R-curves in Fig. 4b and d indicate the range of unstable crack growth. It should be mentioned that these parts are unstable only in the case of a test under monotonously increasing load. In order to allow a more extended part of the R-curve to be determined, special test procedures were developed in the past. One possibility, for instance, is to use a very rigid loading system where the load automatically drops when compliance increases due to crack propagation. A fast piezoelectric loading system also allows reduction of the applied load within a very short response time. So, quasi-stable crack extension is ensured.

If we plot the formally computed stress intensity factor K^*, interpreted as the measured R-curve value, we obtain the solid curves in Fig. 5. At the beginning of unstable crack extension, the related stress intensity factors differ strongly. In experimental studies, the R-curve is mostly computed by Equation 1. The apparent R-curve in terms of K^* starts at a significantly higher value than the correct one and, consequently, is more flat. If we define the starting point of the $K^*(\Delta a)$-curve as K_{I0}, this value becomes much too high. Unfortunately, the true crack tip toughness is never visible in such curves. In order to obtain the true R-curve, we have to measure crack extension for very small cracks at notches and also the notch root radius. Then, application of Equation 2 results in the correct R-curve.

Conclusion: In experimental R-curve investigations crack development usually starts from notches. In the computation of the related stress intensity factors the notch effects are completely ignored in most cases. In the present paper it has been shown that the apparent R-curve computed from the total crack length $a_0 + \ell$ by ignoring any notch effect is too flat. The starting point of the R-curve, K_{I0}, is too high.

References

1. T. NISHIDA, G. PEZZOTTI, T. MANGIALARDI and A. E. PAOLINI, "Fracture Mechanics Evaluation of Ceramics by Stable Crack Propagation in Bend Bar Specimens," edited by R. C. Bradt, D. P. H. Hasselman, D. Munz, M. Sakai, and V. Y. Shevchenko (Fract. Mech. Ceram., 1996) Vol. 11, p. 107.
2. J. KÜBLER, *Ceram. Engin. Sci. Proc.* **18** (1997) 155.
3. T. FETT and D. MUNZ, "Stress Intensity Factors and Weight Functions" (Computational Mechanics Publications, Southampton, 1997).
4. R. DAMANI, R. GSTREIN and R. DANZER, *J. Europ. Ceram. Soc.* **16** (1996) 695.
5. R. J. DAMANI, C. SCHUSTER and R. DANZER, *ibid.* **17** (1997) 1685.
6. E. RUDOLPH, Experimental Results, Reported in [2].
7. A. B. KOUNGA, S. G. YOUSEF, T. FETT and J. RÖDEL, submitted to *J. Amer. Ceram. Soc.*

Received 15 July
and accepted 28 August 2003